

Photoluminescence of excitons bound to isoelectronic B_{80}^4 (1.10680 eV) centers in single-crystal silicon

A. S. Kaminskiĭ and É. V. Lavrov

Institute of Radio Engineering and Electronics, Russian Academy of Sciences, 103907 Moscow, Russia
(Submitted 30 March 1995)

Zh. Éksp. Teor. Fiz. **108**, 1081–1090 (September 1995)

Excitons bound to isoelectronic B_{80}^4 centers, which appear in pure single-crystal silicon (having a density of electrically active impurities $< 10^{13} \text{ cm}^{-3}$) after neutron irradiation followed by annealing at 385 °C, have been investigated. The recombination luminescence spectra of excitons bound to these centers have been investigated in magnetic fields ranging from 0 to 6 T and with uniaxial compression of the samples in the $\langle 001 \rangle$, $\langle 111 \rangle$, and $\langle 110 \rangle$ directions. A high-resolution Fabry–Perot spectrometer has been used for spectral analysis of the recombination luminescence. The fine structure of the ground state of excitons bound to B_{80}^4 centers has been observed. It has been established that the ground state is split in two ($\approx 65 \mu\text{eV}$) and that the optical transition from the lower state is forbidden by the selection rules and appears in the recombination luminescence spectra only in a magnetic field. It has been shown that B_{80}^4 centers are of the trigonal type and have a symmetry corresponding to the C_{3v} point group. The Hamiltonian for excitons bound to B_{80}^4 centers in a magnetic field and in a strain field has been constructed. The structure of the excitonic terms can be explained, if the exchange interaction between the electron and the hole and the interaction of the electron and the hole with the defect potential are taken into account. The splitting of the recombination luminescence lines associated with uniaxial straining of the crystals in the $\langle 001 \rangle$, $\langle 111 \rangle$, and $\langle 011 \rangle$ directions is explained. A comparison of the Zeeman spectra with the results of the calculation yields the g factors of an electron and a hole bound to an isoelectronic B_{80}^4 center, which are equal to $g_e = 2$, $g_{\perp}^h = 2.68$, and $g_{\parallel}^h = 1.27$. © 1995 American Institute of Physics.

1. INTRODUCTION

The investigation of the recombination luminescence of excitons bound to radiation centers is an effective method for obtaining information on their symmetry and composition, as well as on the structure of excitons bound to them.¹ Excitons bound to isoelectronic B_{80}^4 centers¹⁾ have been investigated in a large number of studies. It was shown in Refs. 2–4 that B_{80}^4 centers are of the trigonal type and that excitons bound to these isoelectronic centers have a complex system of excited states and are of the “triplet–singlet” type.^{5,6} In Ref. 7 the radiative decay times of these excitons from the ground and excited states were determined, and it was established that the radiative transition from the triplet state is partially forbidden. We note that the composition of B_{80}^4 centers has not been determined. The purpose of the present work was to obtain additional experimental data using high-resolution spectroscopy, to determine the point group of B_{80}^4 , and to construct a model of an exciton bound to a B_{80}^4 center which would account for the experimental data that has been amassed.

2. EXPERIMENT

Our starting material was pure silicon (the density of electrically active impurities was $< 10^{13} \text{ cm}^{-3}$), which was grown by zone melting without a crucible. The samples were irradiated with neutrons (the cadmium number was ≈ 50) in a $10^{17} \cdot \text{cm}^{-2}$ dose, which corresponds to the addition of

$2 \times 10^{13} \text{ cm}^{-3}$ atoms transmuted into phosphorus to the silicon. Then the samples were subjected to annealing for 30 min in air at a temperature of about 385 °C.

Samples ($10 \times 2 \times 3 \text{ mm}^3$) were cut along the $\langle 001 \rangle$ crystallographic direction, the lateral planes being perpendicular to the $\langle 110 \rangle$ and $\langle 1\bar{1}0 \rangle$ directions, respectively. These samples were used both to obtain the Zeeman spectra and to obtain the dependence of the position and amplitude of the recombination luminescence lines on the direction of the magnetic field. The temperature of the samples could be varied from 4.2 to 1.8 K by evacuating the liquid-helium vapor.

A magnetic field with a strength up to 6.5 T was created in a superconducting solenoid with a central opening having a diameter of 26 mm. When the dependence of the position of the Zeeman components of the recombination luminescence spectrum on the magnetic field strength was recorded, the samples were oriented so that the magnetic field would be parallel to the $\langle 001 \rangle$, $\langle 111 \rangle$, or $\langle 110 \rangle$ crystallographic direction, and when the position and amplitude of the recombination luminescence lines as functions of the magnetic field direction with a fixed magnitude were obtained, the samples were rotated in the $(1\bar{1}0)$ plane from the $\langle 001 \rangle$ direction to the $\langle 110 \rangle$ direction about the $\langle 1\bar{1}0 \rangle$ axis, which was perpendicular to the direction of the magnetic field. The recombination luminescence emitted by the sample perpendicular to the direction of the magnetic field (the Voigt configuration) was subjected to spectral analysis.

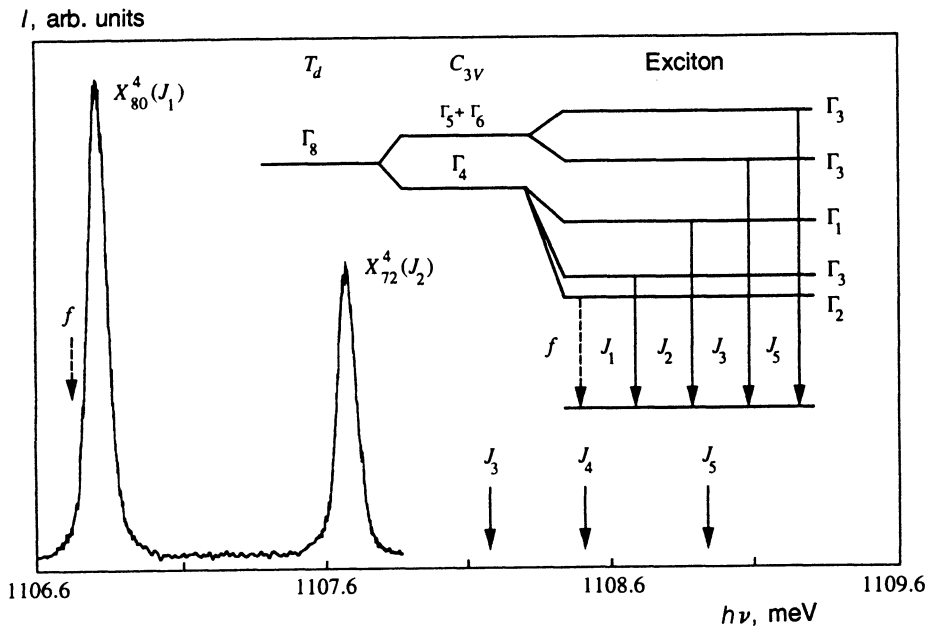


FIG. 1. Spectral distribution of the recombination luminescence of excitons bound to B_{80}^4 centers at 4.2 K. The designations of the lines taken from Ref. 3 are given in parentheses. The arrows in the short-wavelength portion of the spectrum point to the positions of the recombination luminescence lines (taken from Ref. 3) corresponding to excited states. The dashed arrow points to the forbidden transition (f) in the scheme of optical transitions. The inset shows the energy levels of excitons bound to B_{80}^4 , which are labeled by the corresponding irreducible representations in the notation used in Ref. 8. The arrows point to the optical transitions in the ground-state of a B_{80}^4 center (the dashed arrow points to the forbidden transition).

Radiation from an argon laser with a power of ~ 1 W was used to excite the samples. The recombination luminescence was spectrally analyzed using a Fabry–Perot interferometer, in which the spectrum was scanned by varying the pressure of the gas in the chamber. A cooled photomultiplier operating in a photon-counting mode served as the detector of the recombination luminescence. The spectra obtained were recorded with a spectral resolution of ≈ 40 meV.

3. RESULTS AND DISCUSSION

Figure 1 presents a typical spectral distribution of the recombination luminescence of excitons bound to B_{80}^4 centers at 4.2 K. The $X_{80}^4(J_1)$ and $X_{72}^4(J_2)$ lines at 1.10680 and 1.10767 eV correspond to the ground and first excited state of a bound exciton.²⁻⁴ When the temperature is lowered, the contribution of the lines of the ground state increases, and the contribution of the excited states decreases. Conversely, when the temperature is raised, the contribution of the lines of the ground state decreases, and the contribution of the lines of the excited states increases. This is a natural consequence of thermalization. At high temperatures³ the recombination luminescence spectra display two more lines (J_3 and J_5) at 1.10853 and 1.10883 eV (Refs. 2 and 3), which correspond to excited states of an exciton bound to B_{80}^4 . The spectral positions of these lines are indicated in Fig. 1 by arrows. We did not take into account the J_4 line, because it has a low intensity, it was observed only in Ref. 3, and it probably belongs to another center.

Figure 2 presents the evolution of the recombination luminescence spectra of excitons bound to B_{80}^4 in weak magnetic fields. The four spectra in Fig. 2 were obtained at 4.2 K in magnetic fields equal to 0 T (a), 0.29 T (b), 0.49 T (c), and 0.74 T (d). It is seen from Fig. 2 that the X_{72}^4 line, which is assigned to the first excited state of the bound exciton (component 4), does not split in a magnetic field. The X_{80}^4 line, which corresponds to the ground state of the bound exciton,

splits into three components: 1, 2, and 3. Component 1 is absent at zero magnetic field and appears with increasing intensity as the magnetic field is increased from 0 to 0.74 T. Thus, it can be postulated that the ground state is a spin

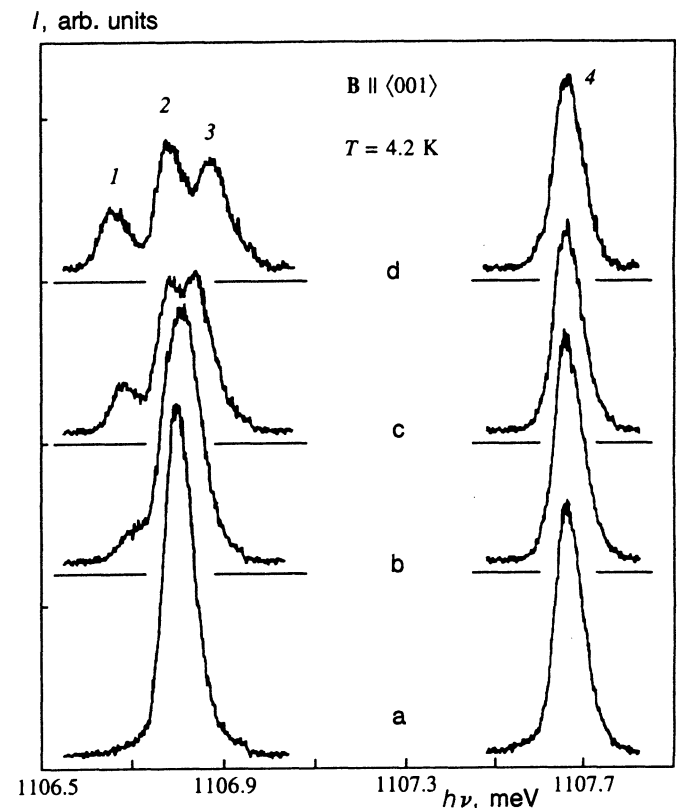


FIG. 2. Recombination luminescence spectra of excitons bound to B_{80}^4 centers obtained in weak magnetic fields at $T=4.2$ K and 0 T (a), 0.29 T (b), 0.49 T (c), and 0.74 T (d) (the Voigt configuration, $B \parallel \langle 100 \rangle$). The numbers label the Zeeman components.

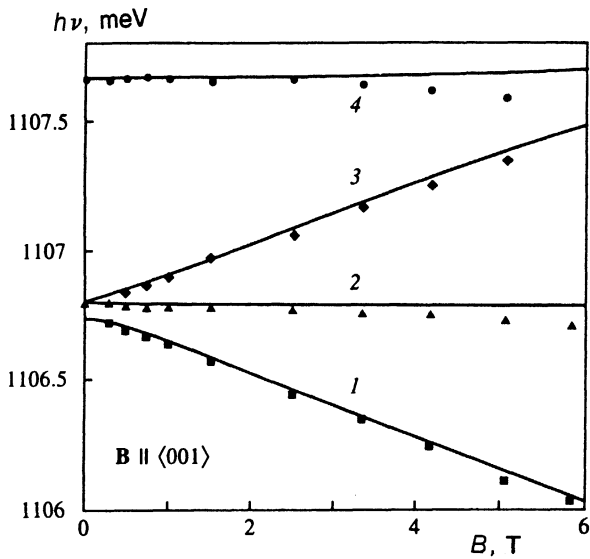


FIG. 3. Dependence of the spectral position of the Zeeman components of the recombination luminescence on the magnitude of the magnetic induction vector \mathbf{B} obtained in the Voigt configuration at $T=4.2$ K with $\mathbf{B} \parallel \langle 001 \rangle$. The circles, diamonds, triangles, and squares mark the empirical positions of the recombination luminescence lines. The solid lines give the positions of the recombination luminescence lines calculated from (1).

triplet, that the first excited state is a spin singlet, and that the exciton bound to B_{80}^4 is of the "triplet-singlet" type²⁾ (Refs. 5 and 6).

Figure 3 presents plots of the spectral positions of individual components of the recombination luminescence spectrum versus the magnetic field strength for $\mathbf{B} \parallel \langle 001 \rangle$ alignment of the magnetic field. As the magnetic field is increased to 6 T, components 2, 3, and 4 are thermalized, and only component 1 remains in the recombination luminescence spectrum (at 2 K). If the magnetic field is aligned parallel to the $\langle 111 \rangle$ or $\langle 110 \rangle$ direction, two components, which correspond to different orientations of the B_{80}^4 defect relative to the crystallographic axes, remain in strong magnetic fields (see Fig. 4) (this is an example of so-called orientational splitting). According to Ref. 9, the number of orientational components just indicated corresponds to a trigonal center.

According to Ref. 9, defects of the trigonal type can belong to two point groups: C_3 and C_{3v} . It was shown in Ref. 5 that the construction of two diagrams is sufficient for determining the point group of a trigonal defect. These diagrams show how the magnitude of the orientational splitting of the recombination luminescence lines of the ground state of the bound exciton and their amplitudes depend on the direction of the magnetic field as it is rotated in the $(\bar{1}\bar{1}0)$ plane. We obtained such diagrams. They are presented in Fig. 4. A qualitative comparison of these diagrams with the diagrams presented in Ref. 5 (see Fig. 4 in Ref. 5) reveals that the B_{80}^4 defect belongs to the C_{3v} symmetry group, and the g factors of excitons bound to it should obey the relation $g_{\parallel} < g_{\perp}$.

Thus, the B_{80}^4 defect is of the trigonal type and belongs to the C_{3v} symmetry point group. We now proceed to a quantitative analysis of the experimental results which we obtained.

All our experimental results can be explained if the model proposed in Ref. 5 for trigonal isoelectronic centers belonging to the C_{3v} point group is utilized. The Hamiltonian for trigonal isoelectronic centers belonging to the C_{3v} point group was derived in Ref. 5 with consideration of a uniaxial strain and a magnetic field. Following Ref. 5, we assume that the potential of the defect splits the quadruply degenerate Γ_8 hole state into two doublets, viz., $\Gamma_5 + \Gamma_6$ and Γ_4 (in the notation used in Ref. 8). The sixfold valley-degenerate electron state splits as a result of the valley-orbit interaction into a Γ_1 (Γ_4 with consideration of the spin) ground state and three excited states, viz., $2\Gamma_3$ and Γ_1 . We also assume that the electron is found in the Γ_1 ground state, which is strongly separated from the excited $2\Gamma_3$ and Γ_1 states. If the electron-hole interaction is now taken into account, a C_{3v} exciton can be found in the following five states:

$$(\Gamma_5 + \Gamma_6 + \Gamma_4)^h \otimes \Gamma_4^e = \Gamma_1^{\text{ex}} + \Gamma_2^{\text{ex}} + 3\Gamma_3^{\text{ex}}.$$

The splitting scheme of the hole and exciton states is pre-

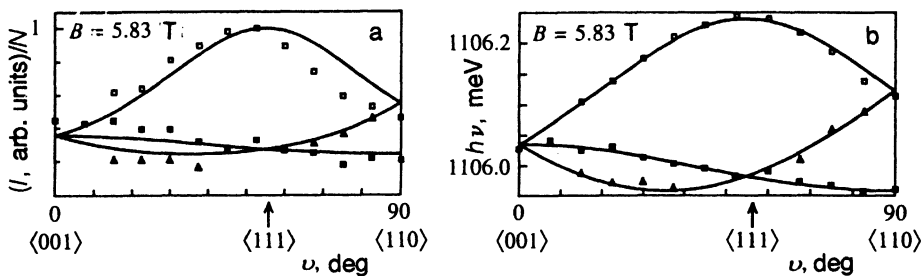


FIG. 4. Dependence of the magnitude of the orientational splitting and amplitude of the recombination luminescence lines corresponding to the ground state of excitons bound to B_{80}^4 centers on the direction of the magnetic induction vector \mathbf{B} with a fixed magnitude $|\mathbf{B}|=5.83$ T. The magnetic induction vector \mathbf{B} was rotated through the angle ϑ in the $(\bar{1}\bar{1}0)$ plane from 0° , which corresponds to the $\langle 001 \rangle$ direction, to 90° , which corresponds to the $\langle 110 \rangle$ direction. The squares and triangles mark the positions of the recombination luminescence lines calculated from (1). $T=2$ K. The arrows point to the angle corresponding to the $\langle 111 \rangle$ direction. N is the degree of degeneracy of the respective exciton state (see the text).

sented in Fig. 1. In order for the long-wavelength transition to be forbidden [as follows from the experiment (see Fig. 2)], the exciton wave function corresponding to this optical transition must transform according to the Γ_2 representation, since the optical transition from Γ_2^{ex} to the Γ_1^{d} ground state of a C_{3V} defect is forbidden [since $\Gamma_1^{\text{d}} \otimes (\Gamma_1^{\text{ph}} + \Gamma_3^{\text{ph}}) \otimes \Gamma_2^{\text{ex}} = (\Gamma_2 + \Gamma_3)$].³ It is seen from Fig. 3 that the first excited state does not split; therefore, the wave function corresponding to it must transform according to the Γ_1 representation. Finally, if we take into account that

$$\Gamma_4^h \otimes \Gamma_4^e = \Gamma_2^{\text{ex}} + \Gamma_3^{\text{ex}} + \Gamma_1^{\text{ex}},$$

it is not difficult to construct the scheme presented in Fig. 1. This scheme agrees well with the data which we obtained. In fact, the ground state has the form of a triplet, one of whose components (Γ_2) is forbidden. The first excited state is a singlet (Γ_1), as is observed in the experiment. The exciton states mix in a magnetic field with the resultant appearance of component 1 (see Fig. 2).

In Ref. 5 we used the theory of invariants¹⁰ to construct the eight-dimensional matrix of the Hamiltonian for a bound exciton belonging to the C_{3V} point group. However, since we were unable to obtain the dependence of the recombination luminescence lines on the magnetic field corresponding to the upper $2\Gamma_3$ exciton terms (see the inset in Fig. 1), we used an approximate Hamiltonian, which can be represented in the form of a four-dimensional matrix.⁵ This Hamiltonian takes into account only the interaction between the three lowest terms (Γ_1 , Γ_2 , and Γ_3), i.e., it neglects the interaction with the upper $2\Gamma_3$ states, and can be represented in the form⁵

$$H = H^0 + H(B). \quad (1)$$

Here

$$H^0 = \Delta_1(\sigma_0 \otimes \sigma_0) + \Delta_2(\sigma_z \otimes \sigma_z) + \Delta_3(\sigma_x \otimes \sigma_x + \sigma_y \otimes \sigma_y),$$

$$H(B) = \frac{1}{2}\mu_B \left\{ g^e \sum_{i=x,y,z} B_i(\sigma_0 \otimes \sigma_i) + g_{\parallel}^h B_z(\sigma_z \otimes \sigma_0) + g_{\perp}^h [B_x(\sigma_x \otimes \sigma_0) + B_y(\sigma_y \otimes \sigma_0)] \right\},$$

where σ_x , σ_y , and σ_z are Pauli matrices, σ_0 is a two-dimensional unit matrix, g^e , g_{\perp}^h , and g_{\parallel}^h are the electron and hole g factors, Δ_k are parameters which determine the energy levels of the exciton in the absence of external perturbations, the B_k are the components of the magnetic field vector, and μ_B is the Bohr magneton.

The positions of the energy levels of the bound exciton were determined by solving the equation

$$\det(H - EI) = 0.$$

We determined the values of the unknown parameters appearing in (1) from the best agreement between the calculation and experiment. In the absence of external perturbations, the energy levels expressed in terms of Δ_1 , Δ_2 , and Δ_3 are at

$$E(\Gamma_1) = \Delta_1 - \Delta_2 - 2\Delta_3,$$

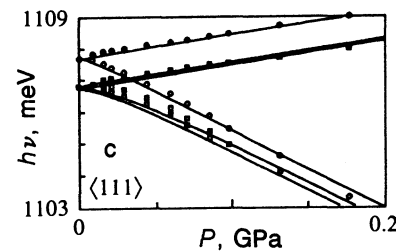
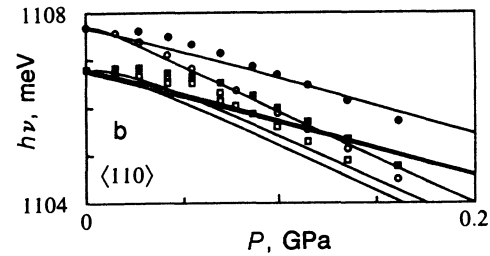
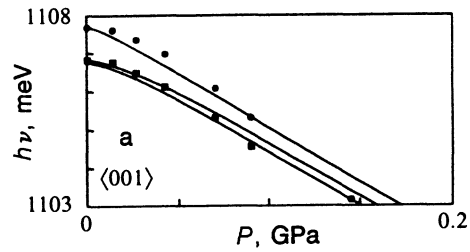


FIG. 5. Splitting of the X_{80}^4 and X_{72}^4 lines under uniaxial compression in the $\langle 001 \rangle$ (a), $\langle 110 \rangle$ (b), and $\langle 111 \rangle$ (c) directions at $T=2$ K. The squares and circles mark the experimental positions of the recombination luminescence lines. The solid curves give the positions of the recombination luminescence lines calculated from Eq. (3).

$$E(\Gamma_2) = \Delta_1 - \Delta_2 + 2\Delta_3, \quad (2)$$

$$E(\Gamma_3) = \Delta_1 + \Delta_2.$$

The values of Δ_k determined from the spectral positions of the J_1 and J_2 lines are $\Delta_1 = 0.27$ meV, $\Delta_2 = -0.2$ meV, and $\Delta_3 = -0.236$ meV.

We determined the values of the g factors in (1) from the best agreement with experiment. Our calculated positions of the lines in the spectra as a function of the magnetic field are shown in Fig. 3. We also plotted the dependence of the orientational splitting of the recombination luminescence lines and their amplitude on the magnetic field strength in Figs. 4a and 4b. To determine the intensities of the lines corresponding to the exciton ground state, we calculated the relative probabilities of the optical transitions $\approx |\langle \Gamma_1 | d | \Psi_i \rangle|^2$, where d is the dipole moment operator and Ψ_i are linear combinations of the Γ_2 and Γ_3 states which diagonalize the Zeeman Hamiltonian. Knowing that the transition from the Γ_2 state is optically forbidden, we can determine the relative intensity of the recombination luminescence line from the exciton ground state in a magnetic field for any orientation of the defect relative to the crystallographic coordinate system. In plots shown in Fig. 4a, the multiplicity N of the orientational degeneracy of each exciton state must be taken into account.

The calculated results thus obtained are shown in the figure as solid curves. The values of the g factors which yield the best agreement with experiment are $g_e=2$, $g_{\perp}^h=2.68$, and $g_{\parallel}^h=1.27$. It is seen from Figs. 3 and 4 that the calculation and experiment agree well.

In conclusion, we consider the influence of uniaxial compression of the samples on the recombination luminescence spectra. As was shown in Ref. 4 (Fig. 5), the recombination luminescence line corresponding to the ground state of the bound exciton (X_{80}^4) splits into three components under uniaxial compression along the $\langle 111 \rangle$ direction, while the line corresponding to the first excited state (X_{72}^4) splits into two components. Such behavior is fully explicable within the proposed model, since no mixing of the Γ_1 , Γ_2 , and Γ_3 exciton states occurs for the centers corresponding to components 1 and 3 under uniaxial compression in the $\langle 111 \rangle$ direction. At the same time, mixing of the exciton states occurs under uniaxial compression for the centers corresponding to components 2, 4, and 5 with the resultant appearance of the forbidden component 5. The behavior of the recombination luminescence lines under uniaxial compression in the $\langle 001 \rangle$ and $\langle 110 \rangle$ directions can be explained in a similar manner. Figure 5 presents the dependences obtained in Ref. 4 of the spectral positions of the recombination luminescence lines with uniaxial compression of the samples in the $\langle 001 \rangle$, $\langle 110 \rangle$, and $\langle 111 \rangle$ crystallographic directions. The solid lines are the results of the calculation we performed. The Hamiltonian which takes into account the interaction of the three lower terms (Γ_1 , Γ_2 , and Γ_3) and the two upper states ($2\Gamma_3$) can be represented in the form of an eight-dimensional matrix H (Ref. 5). We determined the positions of the recombination luminescence lines by solving the equation

$$\det(H - EI) = 0, \quad (3)$$

where

$$\begin{aligned} H &= H^0 + H(\sigma_{kl}), \\ H^0 &= \Delta_1(A_1^1 \otimes \sigma_0) + \Delta_2(A_2^1 \otimes \sigma_z) \\ &+ \Delta_3(E_x^1 \otimes \sigma_x + E_y^1 \otimes \sigma_y) \\ &+ \Delta_4(A_1^2 \otimes \sigma_0) + \Delta_5(A_2^2 \otimes \sigma_z) \\ &+ \Delta_6(E_x^4 \otimes \sigma_x + E_y^4 \otimes \sigma_y), \\ H(\sigma_{kl}) &= \delta_1 \sigma_{zz}(A_1^1 \otimes \sigma_0) + \delta_2(\sigma_{xx} + \sigma_{yy})(A_1^1 \otimes \sigma_0) \\ &+ \delta_3 \sigma_{zz}(A_1^2 \otimes \sigma_0) + \delta_4(\sigma_{xx} + \sigma_{yy})(A_1^2 \otimes \sigma_0) \\ &+ \delta_5(\sigma_{xy} E_x^2 \otimes \sigma_0 \\ &+ (1/2)(\sigma_{xx} - \sigma_{yy}) E_y^2 \otimes \sigma_0) \\ &+ \delta_6(\sigma_{xz} E_x^3 \otimes \sigma_0 + \sigma_{yz} E_y^3 \otimes \sigma_0), \end{aligned}$$

the specific forms of the matrices A and E , which transform according to one-dimensional and two-dimensional representations of the C_{3V} group, are presented in Ref. 5, σ_{kl} is the stress tensor, Δ and δ are experimentally phenomenological constants, the Δ_i specify the positions of the recombination luminescence lines in the absence of external perturbations

and depend significantly on the structure of the center, and δ_i specify the interaction of the exciton with the uniaxial strain field. Note that for uniaxial compression of the samples, we cannot restrict ourselves to the use of the four-dimensional matrix, which leads to positions of the recombination luminescence lines that are linear in the pressure, in contradiction to the experimental data presented in Fig. 5. The nonlinear behavior in Fig. 5 points out a strong interaction of the states considered (Γ_1 , Γ_2 , and Γ_3) with the two upper excited states ($2\Gamma_3$). The parameters appearing in the Hamiltonian H were determined from the best fit between the calculation and experiment. During the fitting, the parameters appearing in (3) were produced by a random-number generator. Since we do not know the dependence of the lines corresponding to the $2\Gamma_3$ excited states, the values presented below for these parameters are arbitrary to a certain extent; nevertheless, as is seen from Fig. 5, the proposed model makes it possible to account for the experimental data quite well. The following values were determined from the optimal fit for the parameters appearing in (3): Δ_1 , Δ_2 , and Δ_3 coincide with the values which we previously determined in Eq. (2), $\Delta_4=1.77$ meV, $\Delta_5=0.33$ meV, $\Delta_6=0$ meV, $\delta_1=-7.7$ meV/GPa, $\delta_2=9.5$ meV/GPa, $\delta_3=-41$ meV/GPa, $\delta_4=4$ meV/GPa, $\delta_5=6$ meV/GPa, and $\delta_6=46$ meV/GPa. Note that δ_6 is similar to the corresponding constant C of a free exciton.¹ However, the values of the δ_i for different centers can differ greatly (for example, $\delta_6=27$ meV/GPa for B_{71}^1), since they depend on the symmetry and the specific form of the wave function of the bound exciton.

4. CONCLUSIONS

In conclusion, we note that the model considered here accounts well for all the experimental findings which pertain to the B_{80}^4 center and are known to us. Attention should also be focused on the surprising similarity of the principal properties of excitons bound to trigonal B_{71}^1 , B_{41} (Ref. 11), and B_{80}^4 centers (the J lines).

This research was performed with partial financial support from the International Science Foundation (grants Nos. MAF000 and MAF300) and INTAS (grant No. INTAS-93-0622).

¹The individual components in the recombination luminescence spectra are labeled by X . The indices accompanying X give the spectral position of the recombination luminescence lines of excitons bound to a B center relative to the bottom of the free-exciton band. For example, the X_{80}^4 line is located 48 meV below the exciton band. The indices accompanying B correspond to the most intense line in the spectrum or the ground-state line. The designations of the same recombination luminescence lines taken from Ref. 3 are given in parentheses.

²Centers at which the ground state of the exciton bound to them is a spin triplet and the first excited state is a spin singlet.

³ Γ_1^d is the irreducible representation according to which the ground state of the defect transforms; Γ_1^{ph} and Γ_3^{ph} are the irreducible representations according to which the dipole moment operator transforms in the C_{3V} group;

the Γ_i^{ex} are the irreducible representations according to which the wave functions of the bound exciton transform in the C_{3V} group.

¹G. Davies, Phys. Rep. **176**, 83 (1989).

²J. A. Rostworowski and R. R. Parsons, Can. J. Phys. **59**, 496 (1981).

³R. Sauer and J. Weber, Physica B **116**, 195 (1983).

⁴A. S. Kaminskiĭ, B. M. Leiferov, and A. N. Safonov, Fiz. Tverd. Tela (Leningrad) **29**, 961 (1987) [Sov. Phys. Solid State **29**, 551 (1987)].

⁵A. S. Kaminskii, E. V. Lavrov, V. A. Karasyuk, and M. L. W. Thewalt, Phys. Rev. B **50**, 7338 (1994).

⁶A. S. Kaminskii, E. V. Lavrov, V. A. Karasyuk, and M. L. W. Thewalt, Phys. Rev. B **51**, 4882 (1995).

⁷A. S. Kaminskiĭ, A. N. Safonov, and É. V. Lavrov, Fiz. Tverd. Tela (Leningrad) **33**, 859 (1991) [Sov. Phys. Solid State **33**, 488 (1991)].

⁸G. F. Koster, J. O. Dimmock, R. G. Wheeler, and H. Statz, *Properties of the Thirty Two Point Groups*, MIT Press, Cambridge, MA, 1966.

⁹A. A. Kaplyanskiĭ, Opt. Spektrosk. **16**, 602 (1964) [Opt. Spectrosc. (USSR) **16**, 329 (1964)].

¹⁰G. L. Bir and G. E. Pikus, *Symmetry and Strain-Induced Effects in Semiconductors*, Wiley, New York; Israel Program for Scientific Translations, Jerusalem, 1974, p. 247 (Russ. original Nauka, Moscow, 1972, p. 394).

¹¹A. S. Kaminskii, E. V. Lavrov, V. A. Karasyuk, and M. L. W. Thewalt, Solid State Commun. (1995).

Translated by P. Shelnitz